Natural fractures and permeability at the geothermal site Rittershoffen, France

Jeanne Vidal[1], Albert Genter[2], Francis Chopin[1], Eléonore Dalmais[2].

[1] EOST, University of Strasbourg, 1 rue Blessig, F-67084 Strasbourg Cedex

[2] ES-Géothermie, 3A chemin du gaz, 67500 Haguenau, France

j.vidal@unistra.fr

Keywords: Natural fractures and faults, permeability, downhole logging methods, acoustic image logs, Enhanced Geothermal System, Rhine Graben, Rittershoffen.

ABSTRACT

A geothermal doublet was drilled at Rittershoffen (Alsace, France) in order to exploit the local geothermal anomaly. Geothermal resource is trapped into fracture network at the sediments-basement interface. Acoustic image logs were analyzed in open-hole section of the wells GRT-1 and GRT-2 and correlated with permeability indication such as temperature anomalies and/or mud losses during drilling operations. The main fracture orientation in GRT-1 is N10°E to N20°E dipping westward. In GRT-2, the main fracture orientation is N160°E to N-S dipping eastward or westward. Less than 5% of fractures present natural permeable indication at borehole scale. Permeable fracture zones present complex cluster indication with major permeable drains surrounded by damage zone.

1. INTRODUCTION

The Upper Rhine Graben (URG) is characterized by several local thermal anomalies associated to hydrothermal convective cells circulating inside a nearly vertical fracture network in the granite basement and in the Triassic fractured sediments above it (Pribnow and Clauser, 2000; Schellschmidt and Clauser, 1996).

A deep geothermal project located at Rittershoffen (Alsace, France) was initiated in 2011 by the company ECOGI, a partnership between the companies Groupe Electricité de Strasbourg and Roquette Frères and the French public financial institution La Caisse des Dépôts et Consignation. The project is based on a geothermal doublet that produces geothermal heat from the reservoir at the sediment-basement interface (Baujard et al., 2015). The heat will be used for industrial processes at the Roquette Frères bio-refinery at Beinheim, located 15 km west of the drill site. A doublet of deep geothermal wells has been drilled to a depth of approximately 2.6 km between 2012 and 2014. It is expected a flowrate of 70kg/s and a surface temperature higher than 160°C (Baujard et al., 2015). The ECOGI project is in commissioning phase and will be operated commercially from summer 2016.

In Enhanced Geothermal Sysems (EGS), multi-scale fracture network acting as fluid pathways is an important component to understand and deal with hard rock reservoirs. Therefore, characterization of natural permeable fracture system at the borehole scale is an important milestone for industrial project.

Standard geophysical logging data, mud logging data and high resolution borehole acoustic image logs have been collected in the deep fractured open-hole sections as well as temperature logs. This work details structural analysis of image logs combined with temperature data and shows the occurrence of permeable local-scale fractured zones or faulted zones developing hydrothermally altered granite called damage zone in both wells. An preliminary attempt to represent the permeable fracture system in 3D is proposed in this study in order to estimate geometrical correlation between the two geothermal wells in their open-hole section.

2. GEOLOGICAL SETTINGS

The project is based on EGS technology and takes advantage of the lessons learned from the Soultz-sous-Forêts geothermal project located less than 10 km to the north-west of Rittershoffen (Figure 1). The doublet was drilled above the so-called Rittershoffen fault. This normal fault is located approximately 15 km east of the Western Rhenane border fault and is oriented N45°E from surface geological data ("Geoportail of EU-Project GeORG - INTERREG IV Upper Rhine," 2012). The open-hole sections penetrated fractured Triassic sandstones, Paleozoic hydrothermally altered granite and fresh granite. The fracture network at the sediment-basement interface was geothermal target of the doublet and showed residual permeability indication. The first well GRT-1 is nearly vertical and its open-hole section is composed by 300 m of sandstones and 350 m of granite. The second well GRT-2 is deviated and its open-hole is composed by 350 m of sandstones and 700 m of granite.

The sandstones are typical medium-grained to conglomeratic continental sandstones with clay

formations called Vosgian sandstones deposited during early Triassic ages. The bottom of the sedimentary cover are argillaceous red sandstones and Permian aged (Aichholzer et al., 2015).

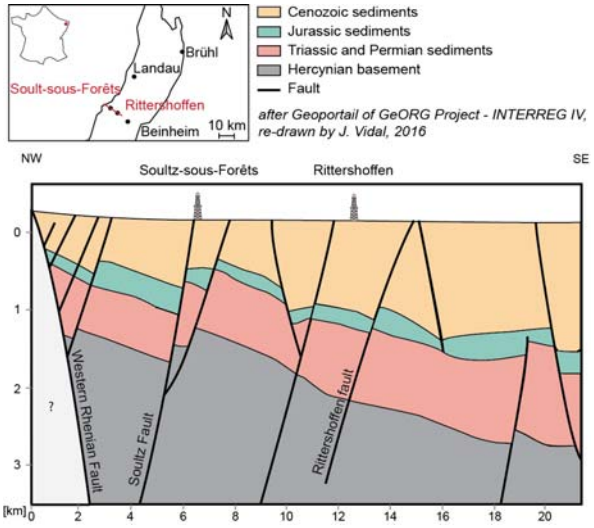

Figure 1: Geological cross-section through Soultz-sous-Forêts and Rittershoffen (after "Geoportail of EU-Project GeORG - INTERREG IV Upper Rhine," 2012).

The Paleozoic granitic basement, encountered at a depth of approximately 2200 m, is divided into three units: the oxidized granite, the hydrothermally altered granite and the fine-grained fresh granite. The Paleozoic granitic basement was affected by pre-Cenozoic tectonics, particularly the Hercynian orogeny. The top of the granitic basement was affected by post-orogenic exhumation and subsequent paleo-weathering. Uplift of the top basement involved an uploading of the rock mass and the formation of low dipping angle fractures called jointing. Residual permeability in the granite is intimately linked to Hydrothermally Altered Fractured Zones (HAFZ) showing a cluster organization deeper in the granitic basement (Genter et al., 2000).

In GRT-1, a preliminary analysis of the natural fracture network and the rock petrography was done from 1400 m to 2600 m (Dezayes et al., 2014). The main fracture orientation is N160°E to N30°E with a main westward dip.

3. MATERIALS AND METHODS

3.1 Description of acoustic image logs

The present study is based on these acoustic image logs, which were produced by Schlumberger and are referred as Ultrasonic Borehole Images (UBIs). This logging was performed using a transducer that emits an ultrasonic pulse towards the borehole wall and records the first echo (Zemaneck et al., 1970). The amplitude and transit time of the reflected signal generate two unwrapped borehole images (Figure 2). The amplitude data correspond to the energy of the reflected signal, i.e., the reflectivity of the borehole wall. The transit time of the pulse from the transducer to the wall and its return is related to the geometry of the borehole and the acoustic velocity in the wellbore mud. The transducer is rotated as it advances, which allows it to create a complete map of the wall as the tool travels a spiral trajectory. An orientation tool consisting of a three-axis inclinometer and a three-axis magnetometer is added to the probe to orient the images with respect to magnetic north (Serra, 2008). It is thereby possible to map the fracture orientations along the well (Davatzes and Hickman, 2005).

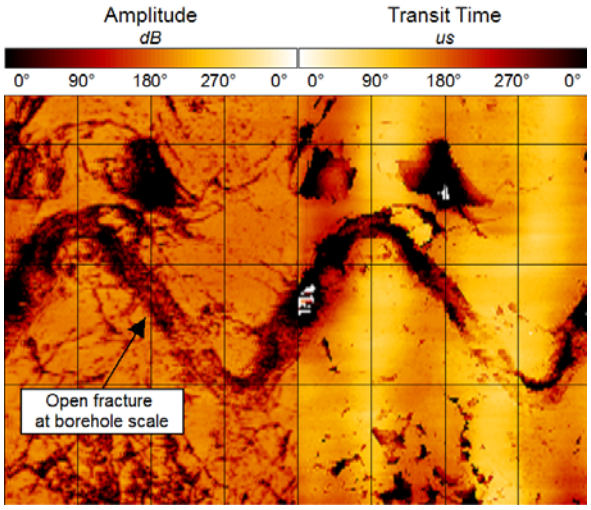

Figure 2: Example of natural fractures from acoustic image logs of the granitic basement in GRT-1.

Natural fractures intersecting the well appear as continuous sinusoidal traces. The amplitude and phase of these traces provide quantitative estimates of their orientations (Figure 2). If this sine wave is also visible in the transit time image (free aperture), then the fracture is interpreted as an open structure at least at the borehole scale. If not, then the fracture is assumed to be completely or partly filled with secondary mineral deposits.

The acoustic image logs of wells GRT-1 and GRT-2 were acquired at a vertical resolution of 1 cm and an azimuthal resolution of 2°. Due to the deviation of the well GRT-2, image log acquisition was affected by "stick and slip" and eccentering effects, especially in the granite when the tool encountered fracture zone cavities (Figure 3). Data quality is lower and 120 m of the open-hole section was not imaged. The bottom hole was not imaged because the well was to hot and the internal temperature tool was critical.

3.2 Fracture characterization

First image log were oriented to the North thanks to the orientation data recorded by the orientation tool. As structural dips picked from image were created in inclined borehole, they were corrected for the inclination and azimuth of borehole trajectories. These corrections provide the true azimuth and dip of fractures.

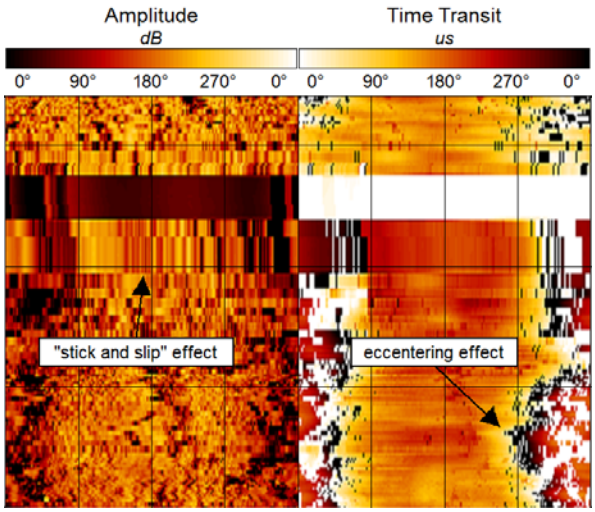

Figure 3: Example of "stick and slip" effect eccentering affecting the acoustic image logs in GRT-2.

In order to summarize the structural orientation information (dip and dip direction) of natural fractures a polar projection diagram (Schmidt diagram, lower hemisphere) is used. Rose diagrams can also be used to represent strikes of the fracture population. In this study, all diagrams represent true dips and dip directions of fractures.

Structural analysis was performed reflecting the lithology (sandstones, oxidized granite, hydrothermally altered granite and fresh granite). Only continuous sine waves were considered in this analysis. The fracture is considered as “major” if its thickness is higher than 1 cm and if transit time data present an aperture (Figure 4). Otherwise the fracture is considered as “minor”. The thickness is the difference of altitude between the depth of the hanging wall and the depth of the foot wall of the fracture. On transit time data, an “acoustic” aperture may be observed. The free aperture of the fracture may be localized on a small section only along the fracture because of presence of secondary minerals.

The permeability of a fracture is assessed if temperature logs present anomalies and/or mud losses are recorded during drilling operations. Negative anomalies on the temperature logs are the thermal signature of permeable fractures that were cooled by the drilling and massive hydraulic injections (Genter et al., 2010). Positive anomalies indicate circulation of hot geothermal fluid through a permeable fracture zone.

4. RESULTS

4.1 Natural fractures in GRT-1

346 natural fractures were observed in GRT-1 among which 19 are considered as major (Table 1). In sandstones, the fracture density is 0.24 fract/m (Figure 5). The main set is oriented N15°E-N20°E with a dip of 80°W (Figure 6). 8 fractures are considered as major but only 1 fracture cluster located in Triassic sandstones is considered as permeable (Table 1). This cluster is composed by 16 fractures belonging to the main fracture set (N20°E, 85°W) and spreading on a 20 m-wide vertical section (Vidal et al., 2016).

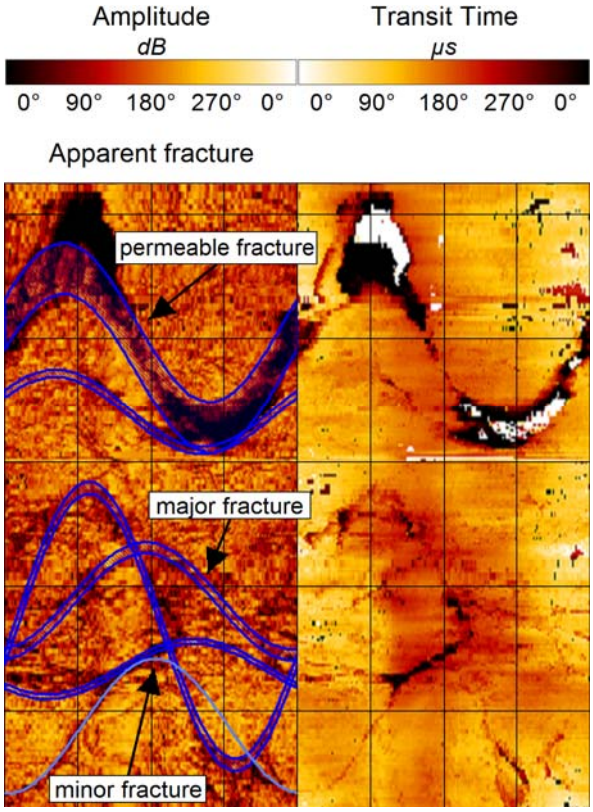

Figure 4: Example of an individual permeable fracture occurring into a fracture cluster affecting the granitic basement in GRT-2.

Table 1: Natural fractures observed in GRT-1 open-hole section from acoustic image logs. Permeable fracture zones are characterized by anomalies on temperature logs and mud losses during drilling operations.

GRT-1		Number of natural fractures	Permeable fracture zones
Sandstones	300 m	68	1
Oxidized granite	50 m	90	0
Deep granite	300 m	188	1
Total	**350 m**	**346**	**2**

At the top of the granitic basement, polar projection is more scattered with two principal directions (Figure 6). One is oriented N15°E-N20°E and dips 50°W-60°W and the other is oriented N160°E-N170°E and dips 55°W-65°W. The highest fracture density of the open-hole section is observed at the top of the granite (2.51 fract/m). They are steeply dipping fractures. Despite of the high fracture density, any fracture presents permeability indication (Figure 5). Only one fracture is considered as major.

The deep granite is divided into two sections: the hydrothermally altered granite and the fresh granite. The fracture density is 0.90 fract/m in the

hydrothermally altered granite and decreases in the fresh granite (Figure 5). 9 out of 112 fractures are considered as major in the hydrothermally altered granite whereas only one out of 76 fractures is considered as major in the fresh granite. Polar projections of fractures in the hydrothermally altered granite and the fresh granite are superimposed. The main fracture orientation is N-S with a dip of 60°W. The set presents an azimuthal scattering from N10°W to N30°E (Figure 6). A minority of fractures are dipping eastward. One permeable fracture zone is observed at the base of the hydrothermally granite (Table 1). The main permeable fracture strikes N175°E, dips 65°W and present a thickness of 24 cm (Vidal et al., 2016). Above this main permeable fracture, from 2325 to 2365 m depth, a 40 m-wide altered and fractured section called damage zone is present.

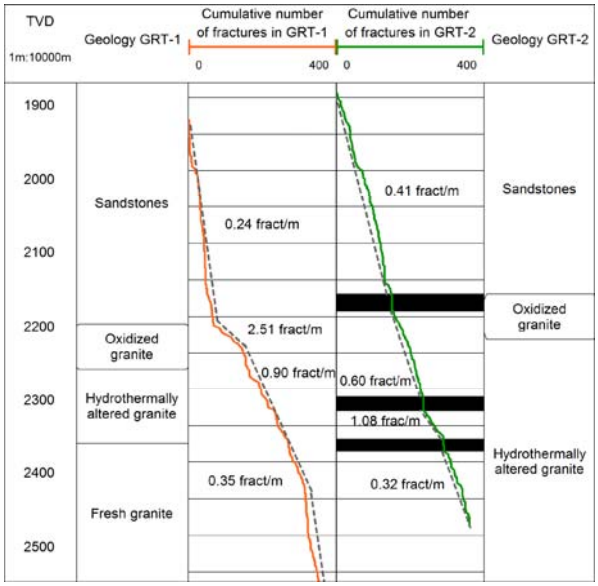

Figure 5: Fracture density in the open-hole section of GRT-1 and GRT-2. Black sections indicate major zones were acoustic images where not acquired. TVD=True Vertcal Depth

4.2 Natural fractures in GRT-2

367 natural fractures were observed in GRT-2 among which 64 are considered as major (Table 2). Fracture orientations are much more scattered in GRT-2 than in GRT-1 (Figure 6).

In sandstones, 142 fractures are observed and 23 are considered as major. The main set is oriented N155°E-N175°E and dips from 80°E to 90°E (Figure 6). This conjugate set presents westward dipping fractures which dip between 50°E and 60°E. Two fracture clusters show permeability indication in both Triassic and Permian sandstones (Table 2). The fracture density is 0.41 fract/m in the sedimentary section of the open-hole.

At the top of the granitic basement, 34 fractures are observed and 7 are considered as major but any one shows permeability indication (Table 2). Fracture orientations are very scattered but the main pole strikes N150°E-N160°E and dips between 60°E and 70°E (Figure 6). In the deep granitic basement, 191 fractures are observed and 44 are considered as major. In the section of hydrothermally altered granite where data were acquired with no sampling artefact, the fracture density is 1.08 fract/m (Figure 5).

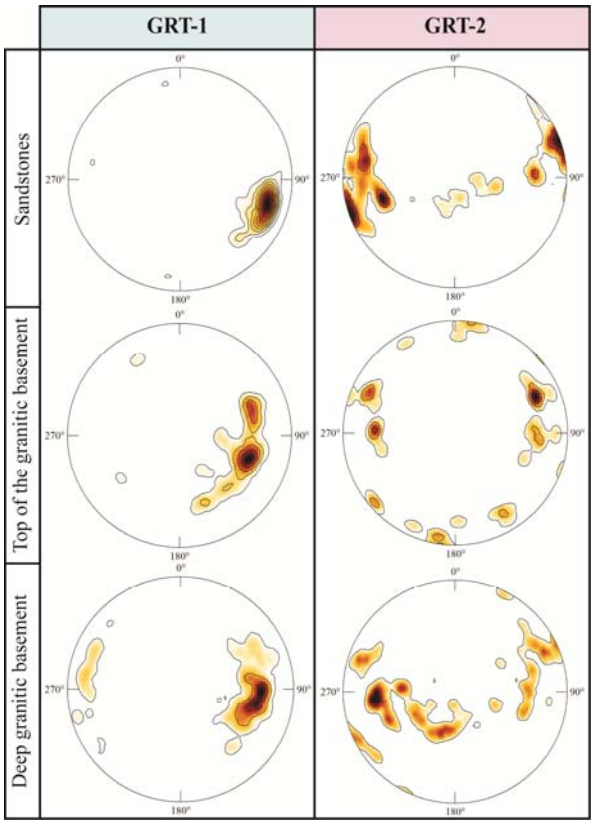

Figure 6: Schmidt diagrams (lower hemisphere) that display density contours of natural fractures in the open-hole section of GRT-1 and GRT-2.

Table 2: Natural fractures observed in GRT-2 open-hole section from acoustic image logs. Permeable fracture zones are characterized by anomalies on temperature logs and mud losses during drilling operations.

GRT-2		Number of natural fractures	Permeable fracture zones
Sandstones	450 m	142	2
Oxidized granite	50 m	34	0
Deep granite	650 m	191	4
Total	**1150 m**	**367**	**6**

The main fracture set strikes N160°E to N-S with dips between 55°E and 65°E (Figure 6). A secondary fracture set strikes N100°E and dips 30°N. Four zones in the hydrothermally altered granite present permeability indication observed in temperature profiles and drilling mud loss occurrences (Table 2). One fracture zone was imaged and correlates with open fracture clusters. It presents a complex structural organization with main permeable fractures surrounding by damage zones extending on several meters. For example, Figure 4 shows a part of a

permeable fracture zone in the hydrothermally altered granite in GRT-2. A main permeable fracture strikes N155°E and dips 80°W and thus belong to the main fracture set. It presents a thickness of 6.5 cm with a partial acoustic aperture. It also correlates with a positive thermal anomaly and mud losses. This fracture intersects another oriented N140°E and dipping 75°W. Below, three major fractures and one minor fracture intersect each other. The major fractures present thickness up to 10 cm and all present acoustic apertures at borehole scale. One of them belongs to the second fracture set with a strike of N78°E and a dip of 27°N. The others belong to the main fracture set with a mean strike of N05°E and a mean dip of 70° W and 30°E.

4.3 Orientation along borehole trajectories

The Figure 7 shows rose diagrams along the open-hole trajectories of GRT-1 and GRT-2 every 150 m-length sections. The GRT-1 trajectory is slightly inclined westward at the bottom hole. At the top of the open-hole section the main direction is N10°E to N20°E associated to sandstone formation (rose diagrams 1.1 and 1.2 Figure 7). At the top of the granitic basement, the main direction is oriented N-S to N10°E (rose diagram 1.3). In the deep basement (rose diagram 1.4), the main direction strikes N30°W to N10°W and a secondary one strikes N10°E. In conclusion, the direction N10°E to N20°E is the most present direction in the open-hole section of GRT-1.

The GRT-2 trajectory is oriented N-S but with a strong deviation of 40°. The top of the open-hole section is dominated by the direction N20°W to N10°W (rose diagram 2.1 Figure 7). The bottom of the sedimentary cover (rose diagram 2.2) presents three main directions very scattered: N20°W and N10°E-N20°E. Secondary directions are N10°W to N30°E.

At the top of the granitic basement (rose diagram 2.3), directions are scattered and strikes mainly N-S, N20°E and N160°E-N170°E. Minor fracture orientations are visble around N70E and N100E. The following 150 m-section (rose diagram 2.4) presents a main direction between N160°E-N170°E as the previous section and secondary directions N-S and N110°E. The deepest rose diagram (2.5) presents three main orientations N-S, N20°E and N160°E-N170°E and two secondary orientations N10°E and N150°E. In conclusion, the angular sector ranging N20°W to N20°E is the most present fracture orientation in the open-hole section of GRT-2.

5. DISCUSSION

5.1 Comparison with regional structural directions

During Variscan orogeny, in the URG area, the main structural trend strikes NE-SW to ENE-WSW. The major Variscan dislocation zone which delimited the Hercynian tectonic realms strikes in that direction (Edel and Weber, 1995; Ziegler, 1990). A further important Variscan trend strikes NNE-SSW.

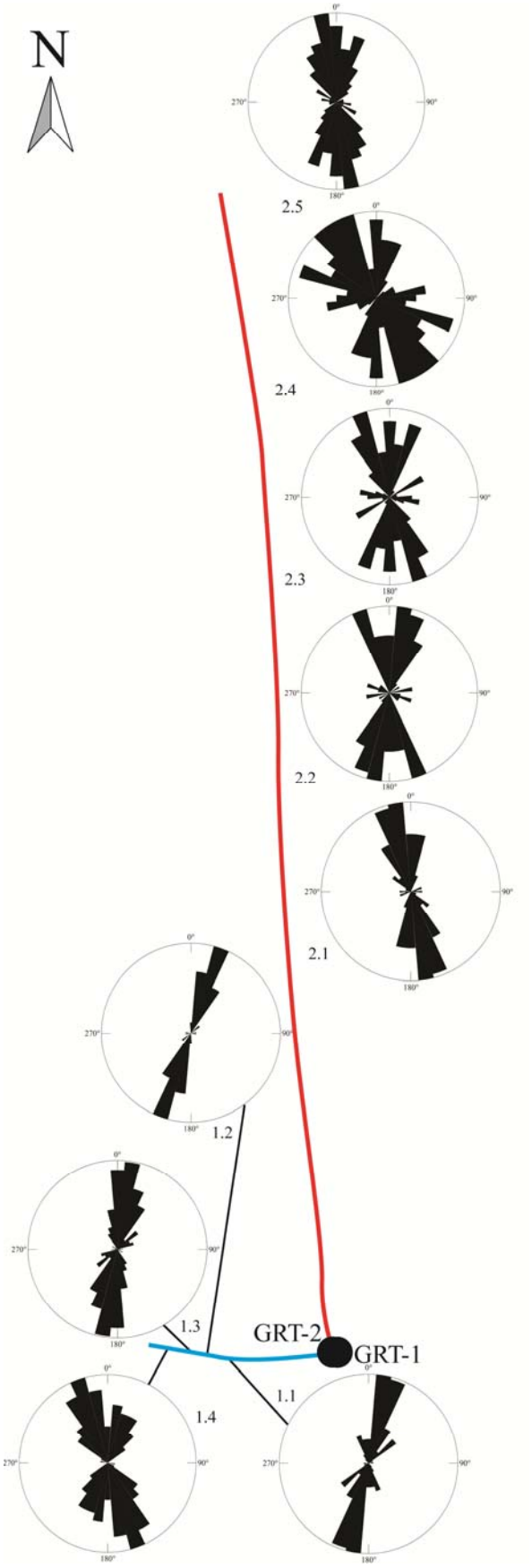

Figure 7: Map of rose diagrams representing natural fracture strikes every 150-m length sections along the open-holes of GRT-1 (in blue) and GRT-2 (in red). Positions of rose diagram are not on scale.

It is also related to sinistral strike-slip fault zones associated with Lower Carboniferous to Permian intrusive bodies and dyke swarms (Edel et al., 2007; Edel and Weber, 1995). The third regional trend strikes N-S to NNW-SSE is associated to these sinistral shear zones. During Eocene rifting phase, a N-S compression is created during the Pyrenean tectonic event and generate dextral shears oriented N160°E to N170°E and sinistral shears oriented N10°E to N20°E. Normal faults forming the URG were created during the Oligocene and strikes N-S to NNE-SSW (Villemin and Bergerat, 1987).

The trend NW-SE is observed in the surroundings of the URG and is associated to dextral faults (Villemin and Bergerat, 1987). During the Cenozoic evolution of the URG, reactivation of a complex set of crustal discontinuities established during Permo-Carboniferous times plays an important role (Schumacher, 2002; Villemin and Bergerat, 1987). Fracture sets in geothermal boreholes and geological outcrops in the URG are associated to the reactivation of old Hercynian structures (Dezayes et al., 2015, 2013). In sediments, predominant orientations in GRT-1 and GRT-2 are consistent with the Oligocene Rhine rifting: NNE-SSW in GRT-1 and also NNW-SSE in GRT-2 (Figure 7). These directions are also present in the granitic basement.

5.2 Comparison with structural directions in Soultz boreholes

Natural fracture orientations where observed in the Soultz geothermal boreholes from core samples, electrical and acoustic image logs. In sandstones, NNW-SSE to N-S-striking and W-dipping fractures dominate (Genter and Traineau, 1996). In the granitic basement, two major families strike N-S and NNW-SSE and dips 75° westward or eastward. Minor families are oriented NW-SE and NE-SW with subvertical dips (Genter et al., 1997; Valley, 2007). In GPK-3 and GPK-4 wells, less than 5% of fractures below 4 km depth strikes E-W and are subvertical or dip 45°S (Valley, 2007).

In sandstones, natural fractures are striking similarly in GRT-2 than in Soultz boreholes with a dip eastward or westward (Figure 6). In GRT-1, fractures strike NNE-SSW and dip westward. In general, fractures in sediments are parallel to the Rhenane direction. This orientation is also major in the granitic basement of Soultz and Rittershoffen.

Horizontal joints present at the top of the granite on core samples in Soultz exploration well called EPS-1 (Genter et al., 1997) are not observed on acoustic image logs in GRT-1 and GRT-2. Maybe, they are not well imaged with this well-logging method because of their low dip. Furthermore fractures at the top of the granitic basement are not associated to large thickness and small fractures below the acoustic image resolution are not detected. In EPS-1 well, the fracture density observed in sandstones on acoustic image logs is the same than in GRT-2. In the granitic basement, the fracture density is higher in Rittershoffen than in Soultz (0.64 fract/m) (Genter et al., 1997).

At Soultz, in the deep granitic basement, maximum horizontal stress is oriented N170°E (Valley, 2007). Natural fractures including the major permeable fracture zones are critically stressed (Evans, 2005). Some major permeable fractures could disturb locally the stress field orientation in the granitic basement (Valley, 2007).

5.3 Fracture network in Rittershoffen boreholes

346 fractures are observed at borehole scale in GRT-1 among which 2 fracture zones are associated to permeability indications. One permeable fracture zone affects Triassic sandstones and one affects granitic basement. 367 fractures are observed at borehole scale in GRT-2 among which 6 fracture zones are associated to permeability indications. Two permeable fracture zones affect Triassic and Permian sandstones, four zones affect granitic basement of which only two were imaged by acoustic image logs. Permeable zones present a complex cluster organization with permeable drains surrounded by altered, porous and fractured zones.

GRT-1 is nearly vertical with a slight deviation westward in the open-hole section. The borehole cross cuts perpendicularly the N-S oriented fracture network which dips westward (Figure 6). The open-hole section was thermally and chemically stimulated in order to improve the injectivity of the well (Vidal et al., 2016). A low pressure hydraulic injection was also performed from the wellhead. The hydraulic behavior is mainly controlled by one originally permeable fault zone at the base of the hydrothermally altered granite. This structure is oriented N170°E. Drilling induced fractures provide an estimation of the maximum horizontal stress orientation in GRT-1 (Hehn, 2016). In GRT-1, the maximum horizontal stress is oriented N15°E in the fractured granite section and rotates from N30°E to N160°E in the deep granitic basement. Variations of maximum horizontal stress orientation in the granitic basement are not clearly associated to the presence of major permeable structures. Analysis of stress field magnitude and orientation in GRT-2 is ongoing work.

GRT-2 trajectory is nearly N-S oriented and highly deviated. Structural analysis at borehole scale indicates that the borehole cross cuts a N160°E to N-S oriented fracture set. Fracture orientations are more scattered and fractures are highly dipping eastward. In the deep granitic basement a minor fracture set is oriented N100°E with low dips (Figure 6). Considering the northward trajectory of the borehole and the high density of N-S oriented fractures that it crosses cut, the borehole was probably drilled into a N-S oriented fracture zone parallel to the open-hole section. In the deep granitic basement, the E-W fracture set was cross cut perpendicularly. The natural flow regime of GRT-2 is controlled by several permeable fracture zones mainly in the granitic

basement. Acoustic image logs show complex permeable fractures belonging to N-S oriented set and E-W oriented set that intersect each other. The well did not required stimulation to reach the expected industrial flowrate. The highly inclined open-hole section of GRT-2 samples more fractures and increases the probability to intersect permeable fracture clusters.

Fracture orientations ranging from N20°W to N20°E are predominant in GRT-1 and GRT-2 regardless of the lithology considered. 3D correlation between fracture zones between GRT-1 and GRT-2 and structural modeling of permeable fracture network will be investigated soon.

6. CONCLUSIONS

Acoustic image logs in open-hole sections of geothermal boreholes GRT-1 and GRT-2 were used to analyze natural fracture network at borehole scale. In GRT-1, fractures are oriented N10°E to N20°E dipping westward. A conjugated fracture system oriented N20°W and N20°E and dipping eastward or westward is observed in GRT-2. Fracture permeability controls fluid circulation through sedimentary and granitic formation. Only 1.2% of fractures are permeable at borehole scale in GRT-1 and 3% in GRT-2. The well GRT-2 intersects a number of permeable fractures more than two times higher than GRT-1. The deviated trajectory of the open-hole section is probably more adapted to geothermal project. The 3D interpretation of fracture network between the geothermal doublet will be investigated soon.

REFERENCES

Aichholzer, C., Duringer, P., Orciani, S., Genter, A., 2015. New stratigraphic interpretation of the twenty-eight-year old GPK-1 geothermal well of Soultz-sous-Forêts (Upper Rhine Graben, France), in: *Proceedings of the 4th European Geothermal Workshop*. Strasbourg, France.

Baujard, C., Genter, A., Graff, J.-J., Maurer, V., Dalmais, E., 2015. ECOGI, a New Deep EGS Project in Alsace, Rhine Graben, France, in: *Proceedings of World Geothermal Congress 2015*. Melbourne, Australia.

Davatzes, N.C., Hickman, S.H., 2005. Comparison of Acoustic and Electrical image logs from the Coso Geothermal Field, CA, in: *Proceedings of Thirtieth Workshop on Geothermal Reservoir Engineering.* Stanford University, California, USA.

Dezayes, C., Lerouge, C., Ramboz, C., Wille, G., 2013. Relative chronology of deep circulations within the fractured basement of the Upper Rhine Graben, in: *Proceedings of World Geothermal Congress 2013*. Pisa, Italy.

Dezayes, C., Lerouge, C., Sanjuan, B., Ramboz, C., Brach, M., 2015. Toward a Better Understanding of the Fluid Circulation in the Rhine Graben for a Better Geothermal Exploration of the Deep Basins, in: *Proceedings of World Geothermal Congress 2015*. Melbourne, Australia.

Dezayes, C., Sanjuan, B., Gal, F., Lerouge, C., 2014. Fluid geochemistry monitoring and fractured zones characterization in the GRT1 borehole (ECOGI project, Rittershoffen, Alsace, France), in: *Proceedings of Deep Geothermal Days. Paris*, France.

Edel, J.-B., Schulmann, K., Rotstein, Y., 2007. The Variscan tectonic inheritance of the Upper Rhine Graben: evidence of reactivations in the Lias, Late Eocene–Oligocene up to the recent. *International Journal of Earth Sciences* 96, 305–325. doi:10.1007/s00531-006-0092-8

Edel, J.B., Weber, K., 1995. Cadomian terranes, wrench faulting and thrusting in the central Europe Variscides: geophysical and geological evidence. *Geol Rundsch* 84, 412–432. doi:10.1007/BF00260450

Evans, K.F., 2005. Permeability creation and damage due to massive fluid injections into granite at 3.5 km at Soultz: 2. Critical stress and fracture strength. *Journal of Geophysical Research* 110.

Genter, A., Castaing, C., Dezayes, C., Tenzer, H., Traineau, H., Villemin, 1997. Comparative analysis of direct (core) and indirect (borehole imaging tools) collection of fracture data in the Hot Dry Rock Soultz reservoir (France). *Journal of Geophysical Research* 102, 15,419-15,431.

Genter, A., Evans, K., Cuenot, N., Fritsch, D., Sanjuan, B., 2010. Contribution of the exploration of deep crystalline fractured reservoir of Soultz to the knowledge of enhanced geothermal systems (EGS). *Comptes Rendus Geoscience* 342, 502–516.

Genter, A., Traineau, H., 1996. Analysis of macroscopic fractures in granite in the HDR geothermal well EPS-1, Soultz-sous-Forêts, France. *Journal of Volcanology and Geothermal Research* 72, 121–141.

Genter, A., Traineau, H., Ledésert, B., Bourgine, B., Gentier, S., 2000. Over 10 years of geological investigations within the HDR Soultz project, France, in: *Proceedings of World Geothermal Congress 2000*. Kyushu - Tohoku, Japan.

Geoportail of EU-Project GeORG - INTERREG IV Upper Rhine [WWW Document], 2012. URL http://www.geopotenziale.org (accessed 4.14.16).

Hehn, R., 2016. Stress field rotation in the EGS well GRT-1 (Rittershoffen, France), in: *Proceedings of European Geothermal Congress 2016.* Strasbourg, France.

Pribnow, D., Clauser, C., 2000. Heat and fluid flow at the Soultz Hot Dry Rock system in the Rhine Graben, in: *Proceedings of World Geothermal Congress 2000*. Kyushu - Tohoku, Japan.

Schellschmidt, R., Clauser, C., 1996. The thermal regime of the Upper Rhine Graben and the anomaly at Soultz. *Zeitschrift für Angewandte Geologie* 42, 40–44.

Schumacher, M.E., 2002. Upper Rhine Graben: Role of preexisting structures during rift evolution. *Tectonics* 21, 6–1.

Serra, O., 2008. *The Well Logging Handbook*, Editions Technip. ed. Paris, France.

Valley, B., 2007. *The relation between natural fracturing and stress heterogeneities in deep-seated crystalline rocks at Soultz-sous-Forêts (France).* PhD thesis, Swiss Federal Institute of Technology Zurich.

Vidal, J., Genter, A., Schmittbuhl, J., 2016. Pre- and post-stimulation characterization of geothermal well GRT-1, Rittershoffen, France: insights from acoustic image logs of hard fractured rock. *Geophys. J. Int.* 206, 845–860. doi:10.1093/gji/ggw181

Villemin, T., Bergerat, F., 1987. L'évolution structurale du fosse rhénan au cours du Cénozoïque: un bilan de la déformation et des effets thermiques de l'extension. *Bulletin de la Société Géologique de France* 8, 245–255.

Zemaneck, J., Glen, E.E.J., Norton, L.J., Cardwell, R.L., 1970. Formation evaluation by inspection with the borehole televiewer. *Geophysics* 254–269.

Ziegler, P.A., 1990. *Geological Atlas of western and central Europe*, 2nd Edition. ed. Shell International Petroleum Mij B V.

ACKNOWLEDGEMENTS

This work was based on data from the ECOGI project at Rittershoffen, France. A part of the work was performed in the framework of the LabEx G-Eau-Thermie Profonde, which is co-funded by the French government under the program "Investissements d'Avenir". A part of this work was done in the framework of the H2020 DESTRESS project which has received funding from the EU Framework Programme for Research and Innovation under grant agreement No 691728. The participation to the EGC 2016 was prepared as a contribution to the PhD thesis of Jeanne Vidal, co-funded by ADEME (French Agency for Environment and Energy). A part of this work was done in the framework of the EGS Alsace project co-funded by ADEME and Electricité de Strasbourg.